Dielectric spectroscopy study on ionic liquid microemulsion composed of water, TX-100, and BmimPF6

Zhen Chen and Ryusuke Nozaki

Citation: J. Chem. Phys. **136**, 244505 (2012); doi: 10.1063/1.4730037
View online: http://dx.doi.org/10.1063/1.4730037
View Table of Contents: http://jcp.aip.org/resource/1/JCPSA6/v136/i24
Published by the American Institute of Physics.

Dielectric spectroscopy study on ionic liquid microemulsion composed of water, TX-100, and $BmimPF_6$

Zhen Chen and Ryusuke Nozaki[a)]
Department of Physics, Faculty of Science, Hokkaido University, Sapporo 060-0810, Japan

(Received 24 January 2012; accepted 5 June 2012; published online 26 June 2012)

We report here a broadband dielectric spectroscopy study on an ionic liquid microemulsion (ILM) composed of water, Triton X-100 (TX-100), and 1-butyl-3-methylimidazolium hexafluorophosphate ($bmimPF_6$). It is found that the phase behavior of this ILM can be easily identified by its dielectric response. The dielectric behavior of the ILM in the GHz range is consistent with that of TX-100/water mixtures with comparable water-to-TX-100 weight ratio. It consists of the relaxations due to ethylene oxide (EO) unit relaxation, hydration water dynamics, and/or free water dynamics. The water content dependence of the EO unit relaxation suggests that this relaxation involves dynamics of hydration water molecules. In the IL-in-water microemulsion phase, it is found that $bmimPF_6$ molecules are preferentially dissolved in water when their concentration in water is lower than the solubility. An additional dielectric relaxation that is absent in the TX-100/water mixtures is observed in the frequency range of 10^7–10^8 Hz for this ILM. This low-frequency relaxation is found closely related to the $bmimPF_6$ molecule and could be attributed to the hopping of its cations/anions between the anionic/cationic sites. © *2012 American Institute of Physics*. [http://dx.doi.org/10.1063/1.4730037]

I. INTRODUCTION

Ionic liquids (ILs) have attracted exploding interest both from academia and industry in the past decades,[1,2] due to their fascinating properties, such as negligible vapor pressure, high thermal stability, nonflammability, and wide electrochemical windows. These properties make them not only an environmentally benign alternative to traditional organic solvents but also a group of advanced materials for diverse purposes like energy storage.[3] Coming along with this explosion of interest are successful applications of ILs in a variety of scientific and technological fields.

Ionic liquid microemulsion (ILM) system has become an attractive topic recently,[4,5] where ILs are used as water substitute, oil substitute, or surfactant. The popularity of this new type of microemulsion is ascribed to its capability of combining the unusual properties of ILs and the versatility of microemulsion. In addition to the "green solvents" nature, ILs are also known as "designer solvents" because their properties can be easily customized by chemical modification or simply pairing ionic species that are available in huge variety.[1] Therefore people can easily prepare task-specific microemulsions through introducing ILs into conventional microemulsions and meanwhile benefit from the green nature of ILs. On the other hand, microemulsions as unique and versatile nanoscale reaction media are capable of expanding the application of ILs into "microscopic environments" as well as offering a more convenient way, as compared to chemical modification, to improve the solubility of ILs in certain chemicals.

A great number of novel ILMs have been prepared in recent years, for example,[6–10] which are subsequently applied with success in materials synthesis, separation, chemical reaction, and so on.[4,5] With the increasing application of ILMs, there is a strong demand of better understanding their physicochemical properties. Although intensive characterization works have been carried out by using a number of techniques, for example, small-angle neutron scattering,[8] UV-Vis spectroscopy,[6,7] and fluorescent probes,[11] their physicochemical properties are still far from being well understood. More characterization methods are highly desired to be employed.

In this study, we use broadband dielectric spectroscopy to characterize a recently prepared ILM composed of water, TX-100, and 1-butyl-3-methylimidazolium hexafluorophosphate ($bmimPF_6$).[6] Dielectric spectroscopy in its modern form has become one of the most effective methods in the characterization of all kinds of materials,[12] because of its many unique properties such as noninvasion, high sensitivity to the fluctuation of dipole moments and ionic motions, and extremely broad frequency range coverage. Although this method has a long and successful history of charactering various microemulsions,[13–17] providing important and sometimes unique information on the microstructure, percolating mechanism, solvation dynamics, etc., not until recently has it been employed to study ILMs.[18,19] In these studies, the phase behavior, the molecular interaction between IL and surfactant, and the percolation mechanism are investigated in terms of the dc conductivity profiles. However, the relaxation behavior of these ILMs is not discussed. In the present study, we will mainly focus on the relaxation behavior of ILM in a wide frequency range. It will be shown that dielectric spectroscopy is effective and convenient in identifying the phase behavior of ILMs; furthermore, it will be also shown that this method is able to provide valuable information regarding issues like the positioning of IL species, the conduction mechanism, and the microstructure of the micelles.

a)Author to whom correspondence should be addressed. Electronic mail: nozaki@dielectrics.sci.hokudai.ac.jp.

II. EXPERIMENT AND METHODS

A. Materials and sample preparation

The ionic liquid 1-butyl-3-methylimidazolium hexafluorophosphate ($bmimPF_6$) was purchased from Tokyo Chemical Industry (Japan) and used without further purification. Triton X-100 (TX-100) was purchased from Sigma-Aldrich and used as received. The number of ethylene oxide (EO) units per TX-100 is about ten. Water was doubly distilled and deionized.

The mixtures of water/TX-100/$bmimPF_6$ were prepared in accordance with the phase diagram of this ternary system at 25 °C.[6] First, the mixture of TX-100 and $bmimPF_6$ with the weight fraction of $bmimPF_6$ being 10% was prepared. After the mixture was fully homogenized, water was added to prepare water/TX-100/$bmimPF_6$ ternary mixtures with different weight fraction of water (ϕ_w): 0.955, 0.901, 0.840, 0.782, 0.721, 0.661, 0.602, 0.520, 0.445, 0.367, 0.304, 0.209, and 0.102. According to the phase diagram, this ternary mixture is in the IL-in-water (IL/water) microemulsion phase when $\phi_w \geq 0.65$, in the bicontinuous (B.C.) phase when $0.33 < \phi_w < 0.65$, and in the water-in-IL (water/IL) microemulsion phase when $\phi_w \leq 0.33$. For simplification these mixtures will be denoted as ILMs hereinafter. To better understand the dielectric behavior of these ILMs, dielectric measurements were also carried out on water ($\phi_w = 1.000$), TX-100/$bmimPF_6$ mixture ($\phi_w = 0.000$), and TX-100/water mixtures with different water content ranging from 10% to 90%.

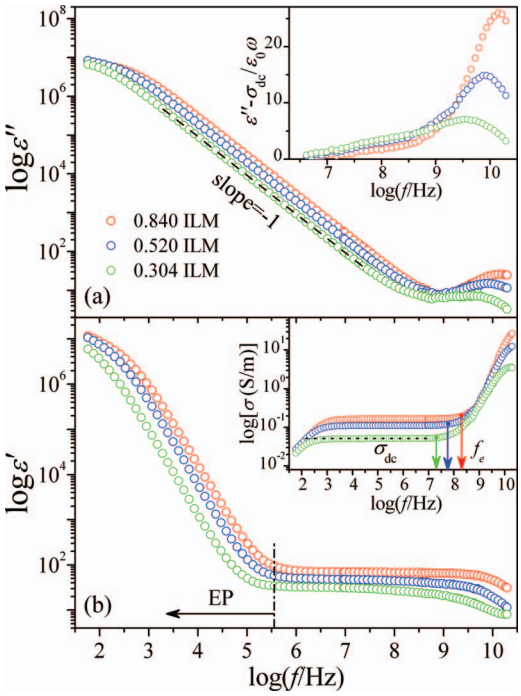

FIG. 1. Frequency dependence of (a) dielectric loss and (b) dielectric constant of 0.840, 0.520, and 0.304 ILMs in the frequency range from 40 Hz to 20 GHz. The insets in (a) shows the frequency dependence of the dielectric loss after subtracting the dc conductivity. The inset in (b) shows the frequency dependence of conductivity, where the arrows indicate the hopping frequency, see text.

B. Dielectric measurement

The complex dielectric permittivity ($\varepsilon^* = \varepsilon' - i\varepsilon''$, where ε' and ε'' are dielectric constant and dielectric loss, respectively) of the samples was measured over a wide frequency range from 40 Hz to 20 GHz. To cover this frequency range, three different experimental setups were used. From 40 Hz to 110 MHz and from 1 MHz to 500 MHz, an impedance analyzer (Agilent 4294A) and a low-frequency network analyzer (HP 4195A) were employed, respectively. For these setups, the values of the complex permittivity were obtained from reflection measurement with a coaxial sample cell located at the end of a coaxial line. The sample cell[17] is composed of an outer conductor with an inner diameter of 3.5 mm and an inner conductor with an outer diameter of 2 mm. The lengths of the inner and outer conductor are 10 mm and 25 mm, respectively. From 200 MHz to 20 GHz, time domain reflectometry[20] was employed, which is coupled with a flat-end capacitor cell[21] using a 2 mm semi-rigid coaxial waveguide. All measurement was carried out at 25 °C with an accuracy of 0.1 °C. The temperature was controlled by using a Compact Ultra Low Temperature Chamber (MC-811, ESPEC Corp., Japan) or by a water jacket[21] connected with a bath that is filled with water/ethylene glycol mixture.

III. RESULTS AND ANALYSIS

A. Dielectric spectra of ILMs

Figure 1 shows the spectra of the complex dielectric permittivity of 0.840 ILM, 0.520 ILM, and 0.304 ILM in the full investigated frequency range, representing the dielectric behavior of ILMs in the IL/water, B.C., and water/IL phase, respectively. The inset in Fig. 1(b) shows the frequency dependence of conductivity σ, which is equivalent to dielectric loss ε'' by the relation $\sigma = \varepsilon_0 \omega \varepsilon''$, where ω ($= 2\pi f$) is the angular frequency and ε_0 is the permittivity of vacuum. A plateau can be observed in the σ spectrum, which in the ε'' spectrum is shown as a linear dependence with a slope of -1 in the same frequency range. The plateau gives the value of dc conductivity σ_{dc} that denotes the value of conductivity in the dc limit. At high frequencies σ begins to increase with increasing frequency. The turning points between this increase and the plateau of σ_{dc}, which are pointed out by the arrows in the inset in Fig. 1(b), correspond to the hopping rates ($\omega_e = 2\pi f_e$) defined in the Dyre theory.[22] The inset in Fig. 1(a) shows the frequency dependence of the dielectric loss after the subtraction of σ_{dc}. Since the contribution of σ_{dc} has been eliminated, the curves in this inset reflect the dielectric loss arising from effective dielectric relaxations.

Due to the existence of $bmimPF_6$, the ILMs are very conductive and large electrode polarization (EP) effect exists. This results in a remarkable increase in ε' with decreasing frequency in the frequency range below 10^6 Hz. Nevertheless, the EP effect has negligible influence on the dielectric relaxations under investigation. Note that the slowest dielectric relaxation occurs in a frequency range higher than 10^7 Hz, as can be seen in the inset in Fig. 1(a), which is far from the frequency range dominated by the EP effect.

Figure 2 shows the frequency dependences of (a) the dielectric constant and (b) the dielectric loss after the

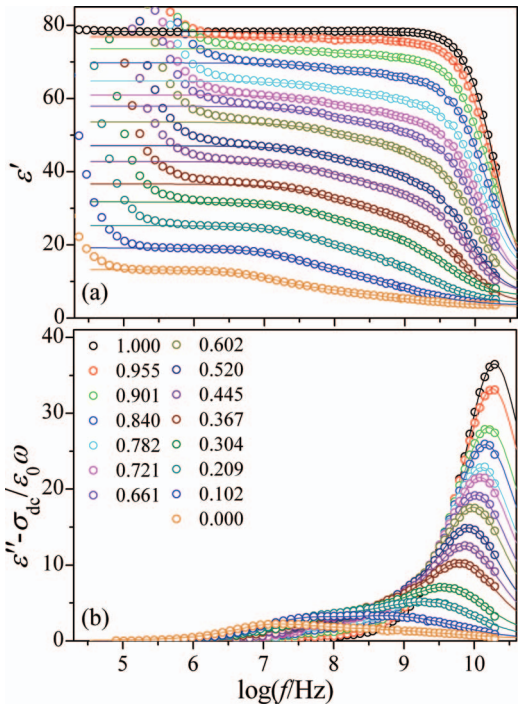

FIG. 2. Frequency dependence of (a) dielectric constant and (b) dielectric loss after subtraction of dc conductivity of water, TX-100/bmimPF$_6$ mixture, and ILMs with different water content. The solid lines are best fits.

subtraction of σ_{dc} of all ILMs in the high frequency range. The dielectric responses of TX-100/bmimPF$_6$ mixture ($\phi_w = 0.000$) and water ($\phi_w = 1.000$) are also plotted in Fig. 2 for comparison. The dielectric behavior of the ILMs seems varying smoothly from the case of water to the case of TX-100/bmimPF$_6$ mixture as water content decreases. At least two dielectric relaxations are visible for the ILMs. The high-frequency dielectric loss peak shifts slightly (within one order) from that of pure water with decreasing water content, which is thereby very likely attributed to the dynamics of water molecules. The low-frequency dielectric loss peak locates in the vicinity of 100 MHz, corresponding to a relaxation with a relaxation time of the order of 1 ns. From Fig. 2(a) one can also notice that these dielectric relaxations are barely influenced by the EP effect; therefore we did not perform elimination of EP effect from the dielectric constant curve.

B. Mechanisms of the relaxations

Because TX-100 molecule contains a hydrophilic chain with about 10 EO units with which water molecules can be associated through hydrogen bonding, the association between water and TX-100 plays a crucial role in the phase structure and chemicophysical properties of TX-100-containing aqueous solutions such as TX-100/water mixtures.[23–26] The dielectric behavior of TX-100/water mixtures in a wide frequency range of 1 MHz to 13.5 GHz was recently investigated by Asami.[23] Obvious dielectric relaxation is observed only above 1 GHz for the mixtures, which is assigned to the dynamics of water molecules including bulk-like (free) water and hydration water. However, relaxations due to the dynamics of micelles[13,27] and due to the radial and tangential diffusion of ions in the micelle/solution interface[15,28] are not observed, although these relaxations have been observed in many micelle solutions. Our measurement results of TX-100/water mixtures are in good agreement with Asami's.

Because the concentration of bmimPF$_6$ is rather low, the ILMs may have similar phase structure to that of TX-100/water mixtures and the dielectric behaviors in both systems may share some common. The dielectric behaviors of ILMs and TX-100/water mixtures with comparable water-to-TX-100 weight ratio are compared in Figs. 3(a)–3(c), and those of TX-100/bmimPF$_6$ mixture and pure TX-100 are compared in Fig. 3(d). It should be pointed out that, although ϕ_w of ILM is a little smaller than that of corresponding TX-100/water mixture, their water-to-TX-100 weight ratios are comparable due to the existence of bmimPF$_6$. As can be seen in Fig. 3, irrespective of the phase composition the dielectric behavior of the ILMs in the frequency range higher than 1 GHz is always consistent with that of TX-100/water mixtures. This implies that the high frequency dielectric relaxation in the ILMs has analogous origin to that in TX-100/water mixtures, namely it is mainly ascribed to the dynamics of water molecules. In the frequency range lower than 1 GHz, a relaxation located in the 10^7–10^8 Hz frequency range can be observed in the ILMs (also in the TX-100/bmimPF$_6$ mixture). However, this relaxation is absent in the TX-100/water mixtures and pure TX-100, suggesting that it arise from the addition of bmimPF$_6$. Considering that the phase structure of the ILMs is similar to that of the TX-100/water mixtures, this relaxation should be closely related to the dynamics of the IL molecules.

A number of other relaxation mechanisms may also contribute to the dielectric relaxations in the frequency range of interest. Generally, they are related to the dynamics of micelles and the diffusion of interfacial ions, as mentioned above. The dynamics of micelles, including the collision and rearrangement, the translational and rotational diffusion, and the thermal shape fluctuation, has a relaxation time of the order of $\eta R^3/k_BT$,[13,27] where η is the viscosity of the dispersing medium, R is the radius of the micelle, k_B is the Boltzmann constant, and T is absolute temperature. For the ILM with $\phi_w = 0.8$, the radius R of the micelle is reported to be 6.3 nm,[6,11] and the viscosity should approach that of the 20% TX-100 aqueous solution (about 0.1 Poise).[29] The relaxation time related to the dynamics of micelle is estimated to be of the order of 600 ns, which largely exceeds the observed relaxation times. The relaxation time of the radial diffusion of the interfacial ions corresponds to the time of the ions diffusing a distance of the order of the micelle radius,[15,28] namely $\tau_r \sim R^2/D \sim 6\pi\eta r R^2/k_BT$ where D and r are the diffusion coefficient and the hydrodynamic radius of the ions, respectively. A rough estimation indicates that it remains in a comparable time scale to that of micelle dynamics; thereby the radial diffusion of the interfacial ions cannot contribute to the observed relaxations either.

The tangential diffusion of the interfacial ions actually arises from the well-known Maxwell-Wagner effect.[15,28] Its relaxation time can be estimated through the following

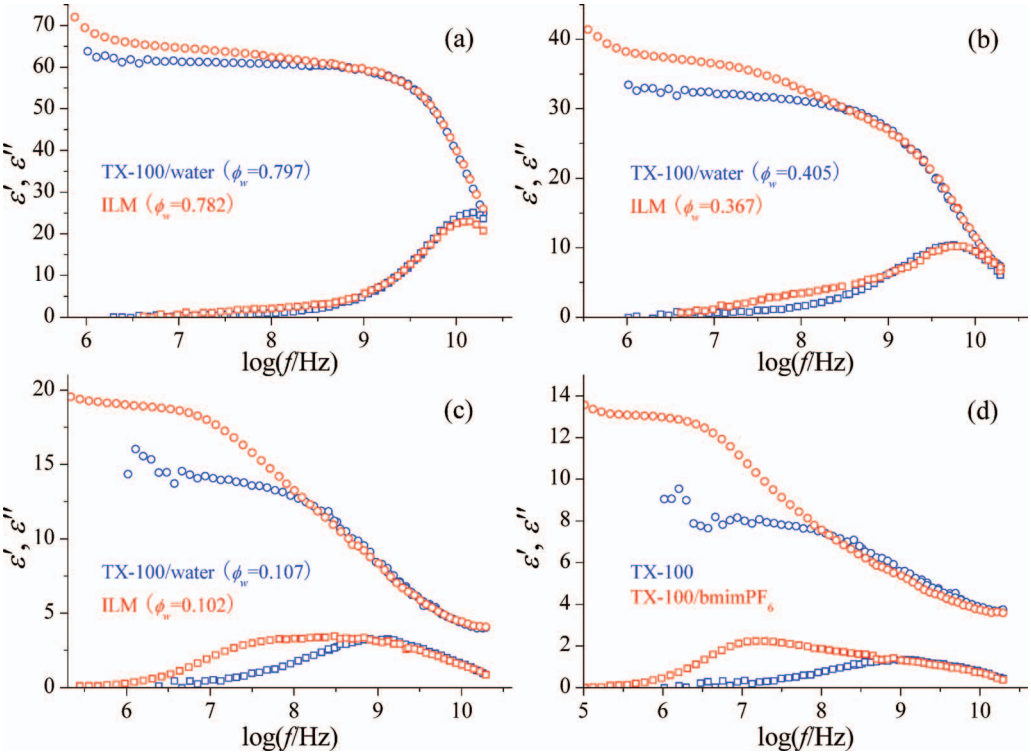

FIG. 3. (a), (b), and (c) The dielectric behaviors of ILMs and TX-100/water mixtures with comparable weight ratio between water and TX-100. (d) The dielectric behaviors of TX-100 and TX-100/bmimPF$_6$ mixture.

equation:[30,31]

$$\tau_{MW} = \frac{2\varepsilon_m + \varepsilon_p + \phi_v(\varepsilon_m - \varepsilon_p)}{2\sigma_m + \sigma_p + \phi_v(\sigma_m - \sigma_p)}\varepsilon_0, \qquad (1)$$

where the subscripts m and p denote the dispersing medium and dispersed particle, respectively, and ϕ_v is the volume fraction of the dispersed phase, which can be converted from the weight fraction of TX-100 by assuming 0.908 cm^3/g for the specific partial volume of TX-100.[23] For IL/water ILMs where aqueous bmimPF$_6$ solution is the dispersing medium and TX-100 micelle is the dispersed particle, $\varepsilon_p = 8$, $\varepsilon_m = 80$, and $\sigma_p \approx 0.005$ S/m (the dc conductivity of the TX-100/bmimPF$_6$ mixture). The dc conductivity of bmimPF$_6$ solution σ_m ranges from 0.17 S/m to 0.65 S/m.[32] A first estimation indicates that τ_{MW} ranges from 4.2 to 1.1 ns in the IL/water phase region, which is in the same order as the relaxation time of the low-frequency relaxation. Therefore, this mechanism is possibly responsible for the low-frequency relaxation, but it cannot contribute to the high-frequency relaxation because even the slowest relaxation process involved in the high-frequency relaxation has a relaxation time of the order of 100 ps (see Table I).

According to the above discussion, the dynamics of the TX-100 micelle and the interfacial ions cannot contribute to the high-frequency relaxation of the ILMs. This relaxation, therefore, should be mainly ascribed to the dynamics of water molecules. The structure and dynamics of water molecules have been extensively investigated by means of dielectric spectroscopy on various aqueous solutions including biological materials,[33–35] polymer,[36–40] and micelles.[15] As demonstrated in these investigations, the relaxations of free and hydration water are generally of the Debye type and always occur at certain frequency, like fingerprint, as long as enough water is present in the system. The relaxation time of free water relaxation is approaching that of pure water (8.3 ps), and the relaxation time of hydration water relaxation is generally 2–3 times larger than that of pure water. For the IL/water ILMs, we have tried to fit the high-frequency relaxation by two Debye processes accounting for the dynamics of the free and hydration water; however it is found that a satisfactory fit can be achieved only if we add another process with a time scale of 100 ps. This indicates that the high-frequency relaxation involves other dynamics in addition to the dynamics of water molecules. A possible dynamics is the motion of the dipoles belonging to the EO units in the hydrophilic chain of TX-100, which has a comparable dipolar size to that of water molecule. This motion has a relaxation time of the order of 200 ps as observed in the aqueous solutions of polyethylene oxide which has a similar local structure to that of TX-100 hydrophilic chain.[39,40] The low-frequency relaxation, on the other hand, is most likely due to the dynamics of the IL molecules but may also arise from the Maxwell-Wagner effect. Detailed discussion on the mechanism of this relaxation is given in Sec. IV.

C. Determination of relaxation parameters

Accordingly, the following fitting function containing three Cole-Cole[41] terms and one Debye[42] term was employed to fit the dielectric spectra of the ILMs and TX-100/water

TABLE I. The fitting results for the different dielectric relaxations observed in water ($\phi_w = 1.000$), TX-100/bmimPF$_6$ mixture ($\phi_w = 0.000$), and ILMs with different water content.

ϕ_w	$\Delta\varepsilon_1$ (±3%)	$\Delta\varepsilon_{EO}$ (±4%)	$\Delta\varepsilon_{hw}$ (±2%)	$\Delta\varepsilon_{fw}$ (±1%)	τ_1(ns) (±1%)	τ_{EO}(ns) (±2%)	τ_{hw}(ps) (±1%)	τ_{fw} (ps)	β_1 (±2%)	β_{EO} (±1%)	β_{hw} (±1%)
1.000				73.15				8.3			
0.955	1.01	0.52	7.98	59.60	1.76	0.136	15.6	8.3	0.78	1	1
0.901	2.31	1.09	17.61	41.05	1.73	0.136	16.3	8.3	0.78	1	1
0.840	3.26	1.72	23.46	30.59	1.60	0.136	15.9	8.3	0.78	1	1
0.782	4.24	2.32	28.45	18.98	1.60	0.137	15.8	8.3	0.78	1	1
0.721	5.14	2.83	30.72	13.73	1.51	0.136	15.6	8.3	0.77	1	1
0.661	5.91	3.25	31.91	7.56	1.49	0.137	16.3	8.3	0.77	1	1
0.602	5.97	3.71	36.15		1.47	0.142	16.0		0.77	1	0.97
0.520	6.39	4.16	30.23		1.55	0.145	18.4		0.77	0.99	0.96
0.445	6.78	4.32	25.15		1.57	0.151	20.3		0.77	0.96	0.95
0.367	7.49	4.49	20.68		1.61	0.156	22.7		0.77	0.95	0.93
0.304	7.29	5.34	13.17		2.00	0.163	32.2		0.79	0.86	0.90
0.209	6.39	8.17	6.82		2.93	0.181	43.1		0.80	0.74	0.87
0.102	5.46	9.35	1.03		5.02	0.229	54.3		0.83	0.66	0.88
0.000	4.56	5.94			18.2	0.339			0.94	0.48	

mixtures:

$$\varepsilon^* = \varepsilon_\infty + \frac{\Delta\varepsilon_1}{1+(i\omega\tau_1)^{\beta_1}} + \frac{\Delta\varepsilon_{EO}}{1+(i\omega\tau_{EO})^{\beta_{EO}}} + \frac{\Delta\varepsilon_{hw}}{1+(i\omega\tau_{hw})^{\beta_{hw}}} + \frac{\Delta\varepsilon_{fw}}{1+i\omega\tau_{fw}}, \quad (2)$$

where ε_∞ is the high-frequency limit of dielectric constant, $\Delta\varepsilon$ is the dielectric increment, τ is the relaxation time, and β ($0 < \beta \leq 1$) is the Cole-Cole parameter indicating the distribution of relaxation time. When $\beta = 1$ the Cole-Cole function goes to the Debye function. The subscripts 1, EO, hw, and fw refer to the low-frequency relaxation, EO unit relaxation, hydration water relaxation, and free water relaxation, respectively.

For the water-rich samples ($\phi_w \geq 0.661$) where free water exists, we found the GHz relaxation can be easily decomposed into three Debye relaxations. The fitting function thus actually contains one Cole-Cole term accounting for the low-frequency relaxation and three Debye terms accounting for the EO unit relaxation and water relaxations. For the water-poor samples ($\phi_w \leq 0.602$), free water relaxation disappears and we found that there exists distribution of relaxation time for EO unit relaxation and hydration water relaxation. Therefore, the fitting function actually contains three Cole-Cole terms. Fig. 4 shows the representative fits for the ILMs in the IL/water (a), B.C. (b), water/IL phase (c), and the fit for the TX-100/bmimPF$_6$ mixture (d). The fitting results of all ILMs are shown in Figure 2, and the values of the fitting variables are summarized in Table I.

IV. DISCUSSION

A. dc conductivity

It is important to mention that it is the ionic species of bmimPF$_6$ rather than the TX-100 micelles that are the dominant charge carriers in the ILMs, as the dc conductivity of the ILMs is more than one order larger than that of TX-100/water mixtures with comparable ϕ_w. The dc conductivity profile of the ILMs therefore reflects the positioning and the microscopic migration environment of the IL species.

Figure 5(a) shows the dc conductivity and the hopping time ($\tau_e = 1/\omega_e$) of the ILMs as a function of water content (ϕ_w). The dc conductivity is determined from the plateau in the σ spectrum. The hopping time, which is the reciprocal of the hopping rate ω_e as exemplified in the inset in Fig. 1(b), represents the time for charge carriers attempting to overcome the highest energy barrier. It can be determined from the σ spectrum through the Dyre formula:[22]

$$\sigma(\omega) = \sigma_{dc}\frac{\omega\tau_e \arctan(\omega\tau_e)}{\{\ln[1+(\omega\tau_e)^2]^{1/2}\}^2 + [\arctan(\omega\tau_e)]^2}. \quad (3)$$

According to the Einstein and Einstein-Smoluchowski relations, dc conductivity is related to the hopping time by[43]

$$\sigma_{dc} = \frac{nq^2\lambda^2}{2k_BT\tau_e}, \quad (4)$$

where n is the effective number density of the charge carriers, q is the elementary electric charge, and λ is the hopping length. For a homogeneous migration environment, this equation gives to the well-known Braton-Nakajima-Namikawa (BNN) relation, namely $\sigma_{dc} \sim 1/\tau_e$.[43] For the present systems, however, dc conductivity should depend not only on the hopping time but also on the IL concentration and the hopping length, because the phase composition changes with water content.

One can find from Fig. 5(a) that the dc conductivity has a nonmonotonic variation with the water content. An inflexion shows up at $\phi_w \approx 0.8$, which is within the IL/water phase region rather than at the phase boundary. While bmimPF$_6$ is generally considered a hydrophobic IL, it has a limited solubility in water (2.1 wt. %).[44,45] For the ILMs with $\phi_w > 0.8$, the weight fraction of bmimPF$_6$ to water is smaller than the solubility, it is thus reasonable to believe that the IL molecules are mostly dissoved in water rather than partitioning into the TX-100 micelles. If this is the case, the bmimPF$_6$ should act as a strong electrolyte in water[44] and the molar conductivity

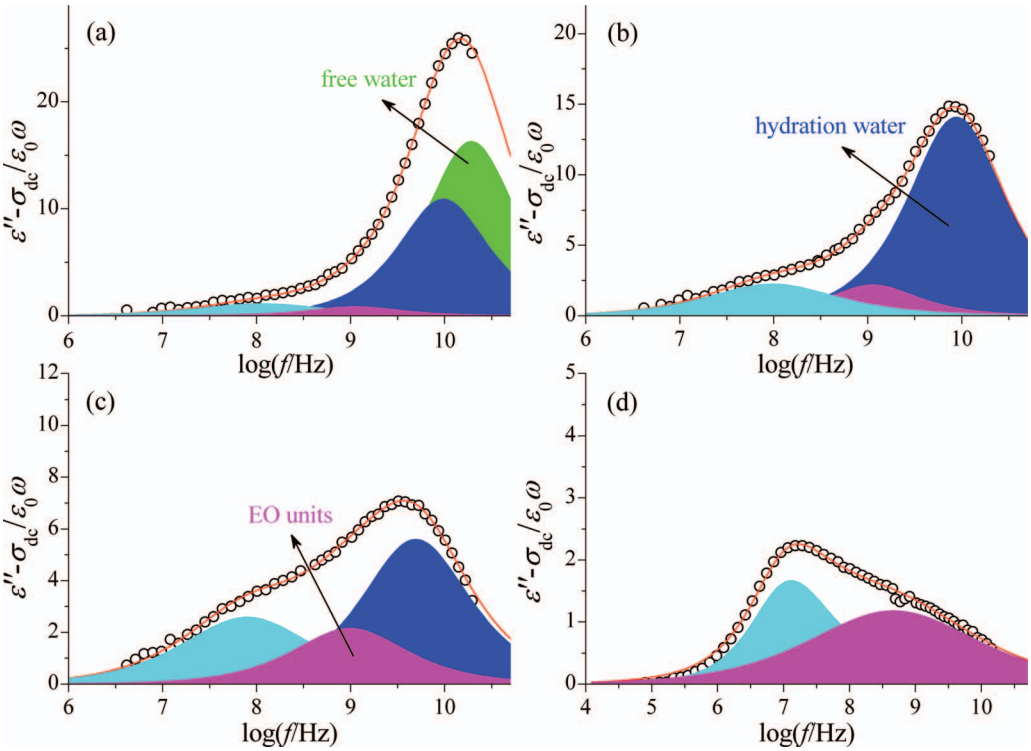

FIG. 4. Fitting results of the dielectric loss curves of (a) 0.840 ILM, (b) 0.520 ILM, (c) 0.304 ILM, and (d) TX-100/bmimPF$_6$ mixture. The solid lines are the total fitting results and the filled area with different color represents the contribution of different relaxation.

(Λ_m) of these ILMs should follow Kohlrausch's square root law given by[46]

$$\Lambda_m = \Lambda_m^0 - \kappa\,[\mathrm{bmimPF_6}]^{1/2}, \tag{5}$$

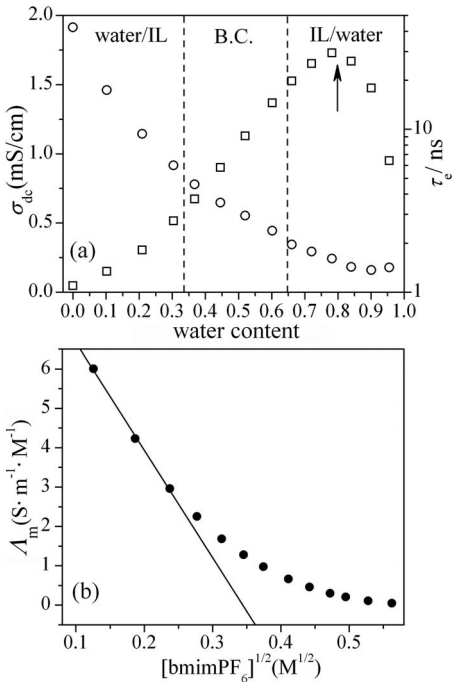

FIG. 5. (a) The dc conductivity (open squares) and hopping time (open circles) of the ILMs as a function of water content. The dashed lines are the phase boundary, and the arrow indicates the inflexion point. (b) The molar conductivity of ILMs as a function of the square root of bmimPF$_6$ concentration. The solid line is the linear fit for the first three concentration points.

where Λ_m^0 is the limiting molar conductivity of bmimPF$_6$, [bmimPF$_6$] is the molar fraction of bmimPF$_6$ in water, and κ is a constant. This equation reveals a linear dependence of Λ_m on $[\mathrm{bmimPF_6}]^{1/2}$. Fig. 5(b) shows the molar conductivity of the ILMs as a function of $[\mathrm{bmimPF_6}]^{1/2}$, from which one can find that the molar conductivity of the ILMs with $\phi_w > 0.8$ (the first three points) basically follows a linear dependence on $[\mathrm{bmimPF_6}]^{1/2}$. The value of Λ_m^0 determined by fitting the first three points in line with Eq. (5) is about 9.41 $\mathrm{S \cdot m^{-1} \cdot M^{-1}}$, which nearly consists with that in dilute bmimPF$_6$ solutions.[44] This result comfirms that bmimPF$_6$ molecules are mostly dissolved in water for the ILMs with $\phi_w > 0.8$.

In the IL/water phase region, τ_e keeps nearly constant when $\phi_w > 0.8$ and increases slightly with decreasing ϕ_w when $\phi_w < 0.8$, as can be seen in Fig. 5(a). Note that the hopping time is plotted in a logarithmic scale. This suggests that the migration (hopping) environments in the IL/water phase are very similar, probably because σ_{dc} mostly arises from the migration of bmimPF$_6$ in water. The hopping length should keep constant in this phase region, and σ_{dc} is thus a function of the effective number density of the IL molecules n_{IL} and the hopping time τ_e according to Eq. (4). When $\phi_w > 0.8$, σ_{dc} increases with decreasing ϕ_w because n_{IL} increases while τ_e keeps constant. When $\phi_w < 0.8$, the concentration of bmimPF$_6$ in water keeps invariable because of saturation, so σ_{dc} decreases with decreasing ϕ_w as τ_e increases. The increase in τ_e with decreasing ϕ_w is possibly due to the increasing intervention of the micelles in the migration pathway of the IL molecules or due to the increase of the viscosity with decreasing ϕ_w.

In the B.C. phase region, the ILM consists of two continuous phases: water phase and TX-100 phase. It is noteworthy that σ_{dc} of TX-100/bmimPF$_6$ mixture is two orders larger than that of pure TX-100, which means the migration of bmimPF$_6$ molecules in the TX-100 phase also gives rise to considerable σ_{dc}. Therefore, it cannot be neglected when one considers the overall σ_{dc} of the ILMs, namely σ_{dc} of the ILMs in the B.C. phase region arises from the migration of bmimPF$_6$ both in the water phase and in the TX-100 phase. Because the hopping time in the TX-100 phase (the case of $\phi_w = 0.000$) is much larger than that in the water phase, the increase of τ_e of the ILMs with the decreasing ϕ_w is mainly due to the growth of the TX-100 phase and meanwhile the diminishment of the water phase. On the other hand, the product of the effective number density and the square of the hopping length $n_{IL}\lambda^2$, which is proportional to $\sigma_{dc}\tau_e$ according to Eq. (4), is found nearly constant in this phase region (see Sec. IV D). Therefore, the decrease of σ_{dc} with decreasing ϕ_w mainly results from the increase of τ_e with decreasing ϕ_w.

In the water/IL phase region, water is confined in reverse micelles and TX-100 is the dispersing medium. The hopping time of the ILMs thus increases more intensely with decreasing ϕ_w as compared with the case in the B.C. phase region. Although $n_{IL}\lambda^2$ decreases slightly with decreasing ϕ_w, the dc conductivity still decreases with decreasing ϕ_w because of the remarkable increase in τ_e.

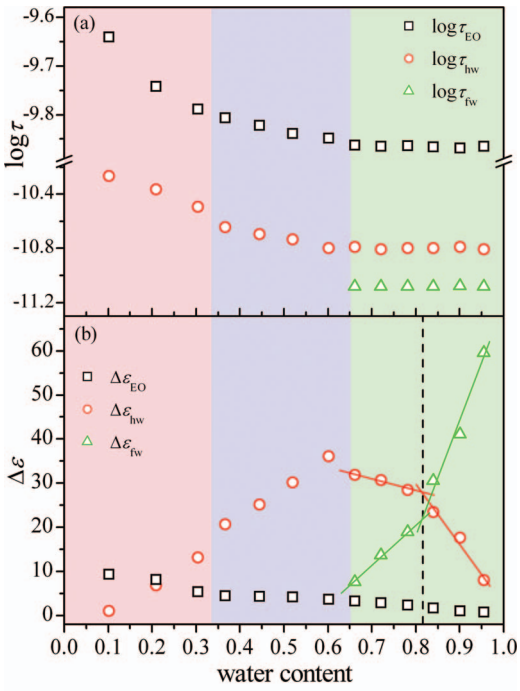

FIG. 6. Water content dependence of (a) the relaxation time and (b) the dielectric increment of the EO unit relaxation (open squares), hydration water relaxation (open circles), and free water relaxation (open triangles). The areas filled with different color represent different phase regions. The dashed line shows the inflexion point, and the solid lines are used for guiding the eyes.

B. Dynamics of water molecules

The dependences of the relaxation time and the dielectric increment of the hydration and free water relaxations on the water content are plotted in Figs. 6(a) and 6(b), respectively. As can be seen, these parameters have different dependence on the water content in different phase regions.

In the IL/water phase region where free water exists, τ_{hw} and τ_{fw} are barely changed with ϕ_w, suggesting the dynamics of water is independent of phase composition. Similar results were also observed in many dilute aqueous solutions. There is no doubt that the faster water dynamics (with smaller relaxation time) is due to the rotational relaxation of free water in bulk. The slower water (with larger relaxation time) relaxation is ascribed either to the rotational relaxation of hydration water molecules or to the exchange of hydration water to free water.[40] The former mechanism is prefered in the present case because this relaxation still exists even though free water is absent. In the B.C. and water/IL phases, free water relaxation disappears and τ_{hw} increases with decreasing ϕ_w. Meanwhile the value of β_{hw} is smaller than uinity in these two phases as shown in Table I, which indicates the distribution of relaxation time and suggests that the relaxation enviroment of hydration water is heterogeneous in the absence of free water. When $0.4 < \phi_w < 0.6$, hexagonal phase with a pocket of lamellar structure is formed in TX-100/water mixtures.[24] The ILMs in the B.C. phase may have a similar microstructure, and in this case the hydration water molecules should be located in a 2D confinement space. This may be responsible for the larger τ_{hw} in the B.C. phase as compared with that in the IL/water phase. In the water/IL phase, water molecules are confined in reverse micelles (3D confinement space), which should be the cause of the more intensive increase in τ_{hw} with decreasing ϕ_w.

In the IL/water phase region, one can see from Fig. 6(b) that $\Delta\varepsilon_{hw}$ increases with decreasing ϕ_w while $\Delta\varepsilon_{fw}$ decreases, which indicates that the concentration of free water molecules are decreasing meanwhile that of hydration water molecules are increasing. This is due to the adding of TX-100 and/or bmimPF$_6$, with which more free water molecules are needed to associate. It is worth noting that an inflexion at $\phi_w \approx 0.8$ also shows up for the ϕ_w dependence of $\Delta\varepsilon_{fw}$ and $\Delta\varepsilon_{hw}$ in the IL/water phase region. As indicated in Fig. 6(b), they are obviously less dependent on ϕ_w when $\phi_w < 0.8$. We believe this is also due to the dissolving state of bmimPF$_6$. When $\phi_w > 0.8$, bmimPF$_6$ molecules are mostly dissolved in water and the association of water with TX-100 is barely influenced by bmimPF$_6$ molecules. As a result, the loss of free water molecules is due to their association with both bmimPF$_6$ and TX-100. When $\phi_w < 0.8$, however, bmimPF$_6$ molecules cannot be dissolved in water any more because of saturation, and the excess bmimPF$_6$ molecules have to be associated with TX-100. Because this association occupies part of hydrogen bounding sites on the hydrophilic chain of TX-100, the effective association between water and TX-100 will be reduced. Therefore, the loss of free water molecules in these ILMs is less intensive than in the ILMs with $\phi_w > 0.8$, and so does the increase of hydration water molecules. This result once more confirms the preceding interpretation on the dissolving state of bmimPF$_6$. It also suggests that bmimPF$_6$ molecues are preferentially located along the hydrophilic tail of the TX-100 molecules rather than within the hydrophobic core of the

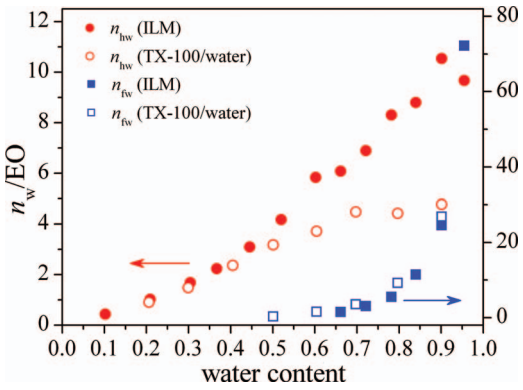

FIG. 7. Water content dependence of the number of water molecules per EO unit for ILMs (filled symbols) and TX-100/water mixtures (open symbols). The circles and squares represent the cases of hydration water and free water, respectively.

micelles, when their concentration in water is larger than the solubility.

Although not strictly, it is generally assumed that the effective mean square dipole moment (μ_{eff}^2) of hydration water molecules is equal to that of free water molecules. The dielectric increment $\Delta\varepsilon$ is thereby a measure of the number density of water moleclues in different association states according to the Kirkwood-Fröhlich equation:[47,48]

$$\Delta\varepsilon = \frac{\varepsilon_s(\varepsilon_\infty + 2)^2}{3(2\varepsilon_s + \varepsilon_\infty)} \frac{\mu_{\text{eff}}^2}{9\varepsilon_0 k_B T} \frac{N}{V}, \tag{6}$$

where ε_s is the static dielectric constant and N is the number of dipoles in a volume of V in the system. The average numbers of hydration and free water molecules per EO unit are roughly calculated by the dielectric increments for ILMs and TX-100/water mixtures, which are compared in Fig. 7.

For water-rich TX-100/water mixtures ($\phi_w > 0.65$), the number of hydration water molecules per EO unit (n_{hw}/EO) keeps nearly constant and its value (about 4.5) is comparable to that obtained in other studies.[23–26] It decreases with decreasing ϕ_w for the mixtures with $\phi_w < 0.65$ because of the decreasing water-to-TX-100 ratio. For ILMs, it should be mentioned that the association of $bmimPF_6$ with water and TX-100 is not taken into account in our calculation on n_{hw}/EO; therefore the calculated value of n_{hw}/EO should somewhat deviate from the real value. Nevertheless, because the concentration of $bmimPF_6$ is small, noticeable deviation of the value of n_{hw}/EO is not expected. From Fig. 7 one can see that n_{hw}/EO of ILMs is much larger than that of TX-100/water mixtures for the samples with $\phi_w > 0.65$. This result means that more water molecules are associated with the hydrophilic chain of TX-100 in the ILMs than in the TX-100/water mixtures and thereby suggests that the size of the micelles in ILMs is larger. The hydrodynamic diameter of the micelles formed in ILMs was recently determined by DLS,[6] which is about 12.6 nm and larger than that of the micelles formed in TX-100/water mixture. The increase in the size of micelles is attributed to the fact that $bmimPF_6$ molecules swell the micelles.

C. EO unit relaxation

The ϕ_w dependences of the relaxation time and the dielectric increment of the EO unit relaxation are also plotted in Figs. 6(a) and 6(b), respectively. One can notice that τ_{EO} has an analogous variation tendency to that of τ_{hw}, which seems implying that the relaxation enviroment of EO unit is similar to that of hydration water or that the EO unit relaxation involves the dynamics of hydration water molecules. The bulk viscosity η of TX-100/water mixtures increases with increasing ϕ_w to a maximum in the range of $0.4 < \phi_w < 0.6$, where gel-like structure is formed, and then decreases with increasing ϕ_w.[29] The bulk viscosity of ILMs should have a similar behavior to that of TX-100/water mixtures considering the rather low concentration of $bmimPF_6$, namely η increases in the IL/water phase but decreases in the water/IL phase as ϕ_w decreases. From Fig. 6(a) one can notice that τ_{EO} keeps nearly constant in the IL/water phase, suggesting that this relaxation is a local relaxation that is not so much related to the bulk properties. Especially in the water/IL phase, where the bulk phase should be mainly composed of TX-100 molecules, τ_{EO} increases with decreasing ϕ_w even though η in this phase decreases with decreasing ϕ_w. Furthermore, the EO unit relaxation is also observed in Pure TX-100 and TX-100/ $bmimPF_6$ mixture (see Fig. 3) in which the concentration of TX-100 is definitely larger than in ILMs and TX-100/water mixtures; however the magnitude of this relaxation in pure TX-100 and TX-100/$bmimPF_6$ mixture is even much smaller than that in ILMs and TX-100/water mixtures. According to these facts, we argue that this relaxation is ascribed to hydrated EO units rather than "dry" EO units. In other words, hydration water, most possibly tightly hydration water, must be involved in this relaxation.

D. The low-frequency relaxation

The low-frequency relaxation should be closely related to the dynamics of $bmimPF_6$ molecules, as mentioned above. The first possible mechanism in this regard that comes to mind is the rotational relaxation of $[bmim]^+$-$[PF_6]^-$ ionic pairs which behave as permanent dipoles. Since $[bmim]^+$ and $[PF_6]^-$ ions can be separately distributed in TX-100 micelle and in bulk water because of different types of interactions between TX-100 and $[bmim]^+$ and/or $[PF_6]^-$,[49] this relaxation is also possibly due to the reorientation of $[bmim]^+$ ions (the dipole moment of $[PF_6]^-$ ion is essentially zero due to the symmetric molecular structure). The hop of cations/anions between the anionic/cationic sites holds another possibility, as it is analogous to the rotation of a permanent dipole.[22,50]

The water content dependence of the relaxation increment ($\Delta\varepsilon_1$) and relaxation time (τ_1) of the low-frequency relaxation is plotted in Fig. 8 and its inset, respectively. One can see that this relaxation has strong dependence on the phase composition. The relaxation time of the low-frequency relaxation can be estimated by the Stokes-Einstein-Debye (SED) theory if this relaxation is due to rotational diffusion:

$$\tau_{rot} = \frac{3V_{\text{eff}}\eta}{k_B T}, \tag{7}$$

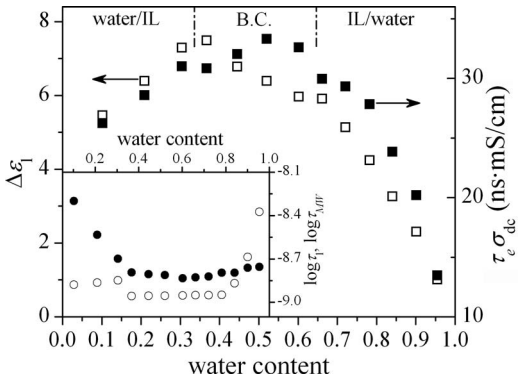

FIG. 8. Water content dependence of the dielectric increment of the low frequency relaxation (open squares) and the product of the hopping time and dc conductivity (filled squares). The inset shows the water content dependence of the relaxation time of the low frequency relaxation (filled circles) and the calculated Maxwell-Wagner relaxation time (open circles).

where V_{eff} is the effective volume of the rotating species. For $[\text{bmim}]^+$-$[\text{PF}_6]^-$ ionic pairs and $[\text{bmim}]^+$ ions, their effective volume is mainly decided by their hydrodynamic radius ($V_{\text{eff}} \sim r_h^3$, r_h being the hydrodynamic radius) and therefore essentially keeps constant. Thus, the rotational relaxation time of these species is only a function of η according to Eq. (7). The inset of Fig. 8 indicates that τ_1 decreases in the IL/water phase but increases in the water/IL phase with decreasing ϕ_w. This variation is opposite to that of η vs. ϕ_w in these phases. Therefore, the low-frequency relaxation cannot be attributed to the rotational relaxation of $[\text{bmim}]^+$-$[\text{PF}_6]^-$ ionic pairs, $[\text{bmim}]^+$ ions, as well as any other species with permanent dipole moment.

Although the hop of cations/anions between the anionic/cationic sites is analogous to the rotation of a permanent dipole, the distance between the anionic/cationic sites is able to change with the phase composition of the system. The relaxation time of this mechanism is thus decided not only by η but also by V_{eff}. If this mechanism is responsible for the low-frequency relaxation, the dielectric increment should be related to the hopping time by[22,50]

$$\omega_e = \frac{1}{\tau_e} = \frac{2\pi\sigma_{\text{dc}}}{\varepsilon_0\Delta\varepsilon}. \tag{8}$$

The value of $\Delta\varepsilon$ calculated from Eq. (8) is about two orders larger than that of $\Delta\varepsilon_1$. The deviation between the calculated $\Delta\varepsilon$ and $\Delta\varepsilon_1$ is possibly arising from the difference in the effective ionic density involved in dc conductance and in this electrical relaxation. The product of the hopping time and dc conductivity ($\tau_e\sigma_{\text{dc}}$) is also plotted in Fig. 8. It can be seen that the variation tendency of $\tau_e\sigma_{\text{dc}}$ is similar to that of $\Delta\varepsilon_1$ over the whole water content range. This result suggests that the low-frequency relaxation has the same underlying mechanism as that of dc conductivity, namely the hop of cations/anions between the anionic/cationic sites. It is also noteworthy that, in the IL/water and B.C. phase regions where water phase is the dominant phase or occupies a considerable portion, the hopping time τ_e is very close to τ_1. In the water/IL phase region, however, τ_e is much larger than τ_1. One should keep in mind that in the water/IL phase region τ_e should be an average hopping time, which may simultaneously originate from a fast migration that involves water molecules and a slow migration in the TX-100 phase. It is thus possible that the low-frequency relaxation in this phase region is mainly a result of the fast migration of the IL cations/anions, noting that $\Delta\varepsilon_1$ in this phase region is decreasing with decreasing water content.

Except for the dynamics of the IL molecules, the Maxwell-Wagner effect may be also responsible for the low-frequency relaxation. The relaxation times of this effect for the ILMs with different water content are calculated in line with Eq. (1), which are also plotted in the inset in Fig. 8. It should be pointed out that, when $\phi_w > 0.8$ the water phase is saturated with bmimPF_6 (about 2.1 wt. %); therefore the dc conductivity of saturated bmimPF_6 solution (around 0.65 S/m)[32] is taken for σ_m (IL/water and B.C. phases) or σ_p (water/IL phase). The values of other parameters are provided above. Attention should also be paid that in the water/IL phase region the dispersed particles are the reverse micelles and the dispersing medium is TX-100/bmimPF_6 mixture. From the inset in Fig. 8 one can find that the Maxwell-Wagner relaxation time is also close to τ_1, but the variation tendency in the water/IL phase region is opposite to that of τ_1. Anyway, this mechanism is still possibly responsible for the low-frequency relaxation or partially contributing to this relaxation.

V. CONCLUDING REMARKS

We have measured the dielectric behavior of a series of water/TX-100/bmimPF_6 ILMs with fixed TX-100-to-bmimPF_6 weight ratio and various water contents (ϕ_w) in a wide frequency range. To better understand their dielectric behavior, dielectric measurements were also carried out on TX-100/water mixtures with various ϕ_w. The comparison of their dielectric behaviors indicates that the dielectric behavior in the GHz range of this ILM is analogous to that of TX-100/water mixture with comparable TX-100-to-water weight ratio. An additional dielectric relaxation located in the frequency range of 10^7–10^8 Hz is observed in the ILMs, which is absent in TX-100/water mixtures.

The mechanism of the GHz dielectric relaxations in the ILMs has been discussed by taking account of the dynamics of water, the EO units, the TX-100 micelles, and the interfacial ions. It is concluded that this relaxation mainly consists of the dynamics of the EO units, the hydration water, and free water, but the dynamics of the micelles and interfacial ions cannot contribute to this relaxation. Detailed analyses are performed on the dielectric spectra based on the relaxation mechanism, by which the dc conductivity and the relaxation profiles, including ϕ_w-dependent relaxation time and relaxation increment, of these dielectric relaxations are obtained. These relaxation profiles clearly reveal the phase transition of this ILM with the variation of ϕ_w, which is well consistent with that characterized by other methods.

The appearance of an inflexion at $\phi_w \approx 0.8$ in the ϕ_w-dependent dc conductivity suggests that bmimPF_6 molecules are preferentially dissolved in water when their concentration in water is lower than its solubility. This is further confirmed by the ϕ_w-dependent dynamics of hydration and free water molecules in the IL/water phase region. The much less intensive dependence on ϕ_w of the water molecule dynamics when

$\phi_w < 0.8$ suggests that bmimPF_6 molecules are located along the hydrophilic chains of TX-100 rather than within the hydrophobic core of TX-100 micelles. As compared with the case of TX-100/water mixtures, the number of hydration water molecules per EO unit in the IL/water phase region of this ILM is obviously larger, suggesting the TX-100 micelle formed in ILM is larger than that in TX-100/water mixtures.

It is also concluded that the low-frequency relaxation observed in this ILM is not a result of the dynamics of TX-100 micelle, the radial diffusion of the surface ions, or the rotational relaxation of $[bmim]^+$-$[PF_6]^-$ ionic pairs or $[bmim]^+$ ions. Since this relaxation is coupled with dc conductivity, it is most likely due to the hopping of IL cationic/anionic species between the anionic/cationic sites. However, the contribution from the Maxwell-Wagner effect to this relaxation cannot be excluded.

ACKNOWLEDGMENTS

This work is partly supported by KAKENHI (Grant No. 19340116), Grant-in-Aid for Scientific Research (B), from the Ministry of Education, Culture, Sports, Science and Technology (MEXT) of Japan.

[1]E. W. Castner, Jr. and J. F. Wishart, J. Chem. Phys. **132**, 120901 (2010).
[2]J. F. Wishart and E. W. Castner, Jr., J. Phys. Chem. B **111**, 4639 (2007).
[3]J. F. Wishart, Energy Environ. Sci. **2**, 956 (2009).
[4]Z. Qiu and J. Texter, Curr. Opin. Colloid Interface Sci. **13**, 252 (2008), and references herein.
[5]T. L. Greaves and C. J. Drummond, Chem. Soc. Rev. **37**, 1709 (2008), and references herein.
[6]Y. Gao, S. Han, B. Han, G. Li, D. Shen, Z. Li, J. Du, W. Hou, and G. Zhang, Langmuir **21**, 5681 (2005).
[7]Y. Gao, N. Li, L. Zheng, X. Zhao, S. Zhang, B. Han, W. Hou, and G. Li, Green Chem. **8**, 43 (2006).
[8]J. Eastoe, S. Gold, S. E. Rogers, A. Paul, T. Welton, R. K. Heenan, and I. Grillo, J. Am. Chem. Soc. **127**, 7302 (2005).
[9]Y. Gao, N. Li, L. Zheng, X. Zhao, J. Zhang, Q. Cao, M. Zhao, Z. Li, and G. Zhang, Chem. Eur. J. **13**, 2661 (2007).
[10]S. Cheng, J. Zhang, Z. Zhang, and B. Han, Chem. Commun. 2497 (2007).
[11]D. Seth, A. Chakraborty, P. Setua, and N. Sarkar, Langmuir **22**, 7768 (2006); J. Chem. Phys. **126**, 224512 (2007).
[12]F. Kremer and A. Schönhals, *Broadband Dielectric Spectroscopy* (Springer-Verlag, Berlin, 2002).
[13]Y. Feldman, N. Kozlovich, I. Nir, and N. Garti, Colloids Surfaces A **128**, 47 (1997).
[14]F. Bordi and C. Cametti, in *Ion Transport and Electrical Conductivity in Heterogeneous Systems: The Case of Microemulsions, Interfacial Dynamics*, edited by N. Kallay (M. Dekker, New York, 2000).
[15]C. Baar, R. Buchner, and W. Kunz, J. Phys. Chem. B **105**, 2906 (2001); C. Baar, R. Buchner, and W. Kunz, J. Phys. Chem. B **105**, 2914 (2001).
[16]C. Cametti, Phys. Rev. E **81**, 031403 (2010).
[17]Z. Chen and R. Nozaki, J. Chem. Phys. **134**, 034505 (2011); Phys. Rev. E **84**, 011401 (2011).
[18]Y. Lian and K. Zhao, Soft Matter **7**, 8828 (2011).
[19]Y. Lian and K. Zhao, J. Phys. Chem. B **115**, 11368 (2011).
[20]R. Nozaki and T. K. Bose, IEEE Trans. Instrum. Meas. **39**, 945 (1990); R. Nozaki, Solid State Phys. (Tokyo) **28**, 505 (1993).
[21]T. Sato, H. Niwa, A. Chiba, and R. Nozaki, J. Chem. Phys. **108**, 4138 (1998).
[22]J. C. Dyre, J. Phys. C **19**, 5655 (1986); J. Appl. Phys. **64**, 2456 (1988).
[23]K. Asami, J. Phys.: Condens. Matter **19**, 376102 (2007).
[24]S. V. Ahir, P. G. Petrov, and E. M. Terentjev, Langmuir **18**, 9140 (2002).
[25]N. Kimura, J. Umemura, and S. Hayashi, J. Colloid Interface Sci. **182**, 356 (1996).
[26]K. Beyer, J. Colloid Interface Sci. **86**, 73 (1982).
[27]Y. Feldman, N. Kozlovich, I. Nir, and N. Garti, Phys. Rev. E **51**, 478 (1995).
[28]C. Grosse, J. Phys. Chem. **92**, 3905 (1988).
[29]See http://dow-answer.custhelp.com/app/answers/detail/a_id/1654 for the information on the viscosity of aqueous solution of Triton X-100 as a function of surfactant concentration at room temperature.
[30]J. C. Maxwell, *A Treatise on Electricity and Magnetism*, 3rd ed. (Clarendon, Oxford, 1891).
[31]K. W. Wagner, Archiv für Elektrotechnik **2**, 371 (1914).
[32]K. Behera, V. Kumar, and S. Pandey, Chemphyschem **11**, 1044 (2010).
[33]S. Mashimo, S. Kuwabara, S. Yagihara, and K. Higasi, J. Phys. Chem. **91**, 6337 (1987).
[34]K. Yokoyama, T. Kamei, H. Minami, and M. Suzuki, J. Phys. Chem. B **105**, 12622 (2001).
[35]A. Oleinikova, P. Sasisanker, and H. Weingärtner, J. Phys. Chem. B **108**, 8467 (2004).
[36]U. Kaatze, O. Göttmann, R. Podbielski, R. Pottel, and U. Terveer, J. Phys. Chem. **82**, 112 (1978).
[37]N. Shinyashiki, Y. Matsemura, N. Miura, S. Yagihara, and S. Mashimo, J. Phys. Chem. **98**, 13612 (1994).
[38]N. Shinyashiki, S. Yagihara, I. Arita, and S. Mashimo, J. Phys. Chem. B **102**, 3249 (1998).
[39]T. Shikata, R. Takahashi, and A. Sakamoto, J. Phys. Chem. B **110**, 8941 (2006).
[40]Y. Satokawa and T. Shikata, Macromolecules **41**, 2908 (2008).
[41]K. S. Cole and R. H. Cole, J. Chem. Phys. **9**, 341 (1941).
[42]P. Debye, *Polar Molecules* (Reinhold, New York, 1929).
[43]J. Sangoro, C. Lacob, A. Serghei, S. Naumov, P. Galvosas, J. Kärger, C. Wespe, F. Bordusa, A. Stoppa, J. Hunger, R. Buchner, and F. Kremer, J. Chem. Phys. **128**, 214509 (2008).
[44]M. Ali, A. Sarkar, M. Tariq, A. Ali, and S. Pandey, Green Chem. **9**, 1252 (2007).
[45]J. L. Anthony, E. J. Maginn, and J. F. Brenneche, J. Phys. Chem. B **105**, 10942 (2001).
[46]P. W. Atkins and J. de Paula, *Atkin's Physical Chemistry*, 8th ed. (Oxford University Press, Oxford, 2006).
[47]J. G. Kirkwood, J. Chem. Phys. **7**, 911 (1939).
[48]H. Fröhlich, *Theory of Dielectrics*, 2nd ed. (Oxford University Press, Oxford, 1958).
[49]K. Behera, P. Dahiya, and S. Pandey, J. Colloid Interface Sci. **307**, 235 (2007).
[50]D. L. Sidebottom, Phys. Rev. Lett. **82**, 3653 (1999).